Grant AFOSR-74-2607E

Catalogue No.
IS ISSN 0072-9310



# PROJECTILE PERFORATION OF MULTI-LAYERED BEAMS

by

I. MAROM and S. R. BODNER

MML Report No. 59

MATERIAL MECHANICS LABORATORY
FACULTY OF MECHANICAL ENGINEERING
TECHNION—ISRAEL INSTITUTE OF TECHNOLOGY
HAIFA, ISRAEL



April 1978

Scientific Report No. 13

prepared for
AIR FORCE OFFICE OF SCIENTIFIC RESEARCH/NA
Building 410, Bolling AFB, D.C. 20332
and
EUROPEAN OFFICE OF AEROSPACE RESEARCH AND DEVELOPMENT
London, England

SECURITY CLASSIFICATION OF THIS PAGE (When Data Entered) UNCLASSIFIED

# REPORT DOCUMENTATION PAGE

READ INSTRUCTIONS BEFORE COMPLETING FORM

| | |
|---|---|
| 1. REPORT NUMBER: AFOSR-TR-78-1100 | 2. GOVT ACCESSION NO. |
| 3. RECIPIENT'S CATALOG NUMBER | |
| 4. TITLE (and Subtitle): PROJECTILE PERFORATION OF MULTI-LAYERED BEAMS | 5. TYPE OF REPORT & PERIOD COVERED: INTERIM rept. 1977-1978 |
| 6. PERFORMING ORG. REPORT NUMBER: MML Report No 59 | |
| 7. AUTHOR(s): I. MAROM, S. R. BODNER | 8. CONTRACT OR GRANT NUMBER(s): AFOSR-74-2607 |
| 9. PERFORMING ORGANIZATION NAME AND ADDRESS: TECHNION-ISRAEL INSTITUTE OF TECHNOLOGY, MATERIAL MECHANICS LABORATORY, HAIFA, ISRAEL | 10. PROGRAM ELEMENT, PROJECT, TASK AREA & WORK UNIT NUMBERS: 2307B2, 61102F |
| 11. CONTROLLING OFFICE NAME AND ADDRESS: AIR FORCE OFFICE OF SCIENTIFIC RESEARCH/NA, BLDG 410, BOLLING AIR FORCE BASE, D C 20332 | 12. REPORT DATE: Apr 78 |
| | 13. NUMBER OF PAGES: 42 (45p.) |
| 14. MONITORING AGENCY NAME & ADDRESS(if different from Controlling Office) | 15. SECURITY CLASS. (of this report): UNCLASSIFIED |
| | 15a. DECLASSIFICATION/DOWNGRADING SCHEDULE |

16. DISTRIBUTION STATEMENT (of this Report)

Approved for public release; distribution unlimited.

17. DISTRIBUTION STATEMENT (of the abstract entered in Block 20, if different from Report)

18. SUPPLEMENTARY NOTES

19. KEY WORDS (Continue on reverse side if necessary and identify by block number)

BALLISTICS, TERMINAL
PERFORATION
PENETRATION
IMPACT
MULTI-LAYER
DYNAMIC PLASTICITY

20. ABSTRACT (Continue on reverse side if necessary and identify by block number)

A combined analytical and experimental study has been performed on the ballistic resistance of layered targets, in particular, of flat, relatively thin beam with clamped ends in spaced and laminated (i.e., in contact without bonding) conditions. The theoretical analysis combines the effect of structural deformation with the mechanism of perforation. This requires a redefinition of the ballistic limit velocity as the initial impact velocity for which the post perforation velocity and the structural deformation velocity of the impact point would be equal at the same time. The ballistic tests were based on commercially pure and alloy (6061-T6)

DD FORM 1 JAN 73 1473

401 910

UNCLASSIFIED
SECURITY CLASSIFICATION OF THIS PAGE (When Data Entered)

aluminum target specimens of various thicknesses and configurations, and a 0.22 (in.) caliber projectile which struck the targets perpendicularly at their center with a velocity of 375 m/s. The results for the velocity drop show fairly good agreement between experiments and predictions, and greater ballistic resistance of the laminated configuration.

# PROJECTILE PERFORATION OF MULTI-LAYERED BEAMS

by

I. Marom[1] and S. R. Bodner[2]

Faculty of Mechanical Engineering

Technion - Israel Institute of Technology

## Abstract

A combined analytical and experimental study has been performed on the ballistic resistance of layered targets, in particular of flat, relatively thin beams with clamped ends in spaced and laminated (i.e., in contact without bonding) conditions. The theoretical analysis combines the effect of structural deformation with the mechanism of perforation. This requires a redefinition of the ballistic limit velocity as the initial impact velocity for which the post perforation velocity and the structural deformation velocity of the impact point would be equal at the same time. The ballistic tests were based on commercially pure and alloy (6061-T6) aluminum target specimens of various thicknesses and configurations, and a 0.22 (in.) caliber projectile which struck the targets perpendicularly at their center with a velocity of 375 m/s. The results for the velocity drop show fairly good agreement between experiments and predictions, and greater ballistic resistance of the laminated configuration.

---

[1] Graduate Student (formerly)

[2] Professor

## Introduction

Multi-layered shielding for protection against ballistic perforation is employed for certain applications where it is considered to be advantageous over monolithic structures. In the case of hypervelocity impact by meteoroids, for example, an outer shield could serve to break the projectile into fragments before it hits the main structure, e.g. [1]. The problem of ballistic perforation of multi-layered target plates at standard ordnance velocities, i.e., from about 300 to 1000 m/s, has not received much attention and it complicates the already formidable perforation problem. The current status of this problem for single target plates has recently been the subject of an extensive review by Backman and Goldsmith [2].

For ordinary perpendicular ballistic impact (i.e., impact velocities less than about 1000 m/s) of ductile targets, it is not obvious that separate layers have an advantage over a monolithic plate of equal weight. A limited number of results on multi-layered targets is available in the literature, e.g. [3,4,5], and some interesting observations have been made, but general conclusions are difficult to formulate on the basis of special cases and materials. At moderate impact velocities, it would appear that layered plates in contact should be advantageous over similar separated layers, but it is not certain that they have more resistance than equivalent monolithic plates. Maintenance of contact between layered plates increases the effect of the compressive force acting on the projectile which leads to its greater deceleration and also to its flattening. Comparing laminated (in contact) to monolithic targets, the former

have lower shear resistance but are more conducive to overall deformation (also referred to as bulging and dishing) which can be a significant energy absorbing mechanism. Whichever effect dominates in particular cases would indicate the relative advantage.

An important aspect in analyzing the multi-layered target problem is the interaction of the perforation process with overall structural deformation. Previous studies on the topic have considered these as essentially uncoupled effects, e.g. [6,7,8,9]. At high velocities relative to the ballistic limit, the time for perforation is short compared to that of structural response, so bulging could be considered a late stage consequence of the impulse imparted by perforation. Alternatively, at low velocities the structural response of the target plate is considered as an initial stage preceding possible perforation.

A coupled perforation-bending analysis of clamped beam targets is developed in the current paper. It is based on the ballistic perforation theories of Recht and Ipson [10] and Awerbuch and Bodner [11,12] and the dynamic plastic beam bending theory of Parkes [13,14]. Beams consisting of flat, relatively thin flat strips of aluminum with clamped ends were chosen for the targets to somewhat simplify the analysis and the associated experiments, but similar results should apply for plate targets under the appropriate test conditions and corresponding analyses. For plates, analyses such as those of Beynet and Plunkett [7] or Dienes and Miles [8] for the plastic membrane response of impacted plates would substitute for the plastic beam bending results of Parkes. As in the above references, the

effects of elastic and plastic wave propagation and of friction and heating are not considered in this investigation.

An experimental program was conducted in conjunction with the analysis to guide the theoretical development and to supply results for comparison. The beam specimen materials were 1100-H14, 1100-H16, and 6061-T6 aluminum, and an ordinary 0.22 (in.) caliber lead bullet was the projectile. High speed photographs were taken to supply information on the perforation process, the residual velocity, and the perforation time.

As expected, layered targets in contact has superior ballistic resistance over spaced layers in this particular application. There was also some advantage of the laminated (in contact) beams over monolithic targets of equivalent thickness due to the overall bending effect. Optimizing the number and thicknesses of the layers for a given total thickness could probably be achieved on the basis of the developed analysis, but this was not attempted here.

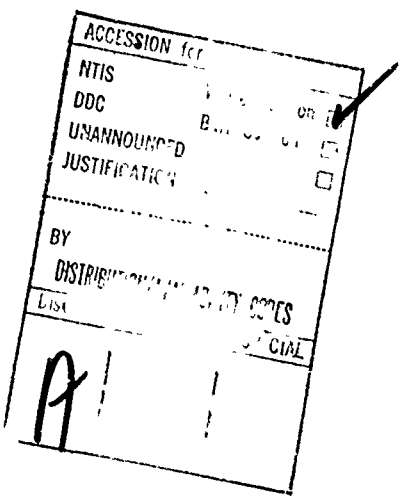

## Analysis

An unresolved problem in the investigation of ballistic perforation of multi-layered as well as uniform target plates is the interaction between overall structural deformation and the localized mechanism of perforation. A parameter that could combine these effects is the ballistic limit velocity which is the minimum impact velocity required for perforation, or, alternatively, the maximum impact velocity corresponding to zero residual velocity. The ballistic limit velocity is an essential parameter in the energy balance equation of ballistic perforation [10].

A method for considering structural deformation effects in the mechanism of perforation is to redefine the ballistic limit velocity as the impact velocity for which the residual velocity equals the structural response velocity at the impact point. That is, the ballistic limit is reached when the relative velocity between the exiting projectile and the structural movement at the impact point becomes zero. More precisely, the ballistic limit velocity could be calculated as the initial impact velocity such that the residual velocity obtained from the kinetic equations of perforation [11] would be equal to the impact point motion according to rigid-plastic beam theory [13,14], (or appropriate dynamic plate response theories, e.g. [6,7,8]). The time for perforation obtained from [11] would be the time at which the structural motion is calculated. With the ballistic limit velocity known, the momentum and energy balance equations of [10] serve to obtain residual velocities for higher impact velocities.

In applying this concept to multi-layered targets, it is convenient to consider each layer individually during the perforation process. Downstream layers would have no effect on the current impacted layer for separated beams, while the main influence of laminated but unbonded systems would be to generate an additional compressive force on the projectile-plug system. This compressive force leads to greater flattening of the projectile and to an additional work term in the energy balance euation.

For independent, separated layers, the energy balance relation for the residual velocity of a single layer is given by eq. (5) of [10], which, in slightly modified form is

$$V_r = \left[ \frac{V_i^2 - V_L^2}{(1 + \frac{m_e}{m_i})(p + q\,\frac{m_e}{m_i})} \right]^{1/2} \qquad (1)$$

where

$V_r$ = residual velocity (of current layer)

$V_i$ = impact velocity of projectile (for current layer)

$V_L$ = ballistic limit velocity (of current layer)

$m_e$ = total mass of material ejected from layer = $\pi d^2 h \rho / 4$

$m_i$ = total mass of projectile prior to impact of current layer (including material ejected from previous layers)

$p$ = fraction of initial projectile mass after fragmentation losses

$q$ = fraction of ejected material mass moving with projectile after fragmentation losses

$d$ = current diameter of projectile and ejected mass (assumed constant within each (thin) layer)

$h$ = thickness of current layer

$\rho$ = mass density of target material

In practice, the coefficients p and q were found in the associated experimental program to be close to unity and $p = q = 1$ was used in the calculations. A procedure for predicting projectile flattening with penetration distance is not available so d has to be determined by direct experimental observation or from empirical information.

When the target layers are in contact, the energy balance relation should include the work performed on the supporting layers during the plugging process. This would be the work done by the ultimate compressive stress $\sigma_c$ acting on the plug area $\pi d^2/4$ over the distance of the layer thickness h. The stress, $\sigma_c$, is considered to be constant during the perforation process, so $V_r$ for this case is given by

$$V_r = \left[ \frac{V_i^2 - V_L^2}{\left(1 + \frac{m_e}{m_i}\right)\left(p' + q' \frac{m_e}{m_i}\right)} - \frac{\sigma_c \pi d^2 h}{2(p' m_i + q' m_e)} \right]^{1/2} \qquad (2)$$

The mass coefficients p' and q' could, in principle, be different in this case, but were observed to be also close to unity for the associated experiments. For the last layer in a sequence of layers in contact, the compressive stress effect would be absent so eq. (1) would be applicable. Because of added projectile flattening due to

the compressive stress, the values of d for layers in contact would be greater than for equivalent separated layers.

It is noted that eqs. (1) and (2) include the effects of structural motion in the parameter $V_L$ and indirectly by inclusion of a peripheral shear energy term which transforms into kinetic energy of the layer. In using eq. (1) or (2) for each layer, it is necessary to consider the current projectile diameter d due to flattening and the current effective mass of the projectile taking account of material added from the previous layers. The ballistic limit velocity $V_L$ would therefore be different for each layer. Generally, the material, thickness, and spacing of the layers could be varied but the same material, layer thickness, and spacing were used in each individual target in this investigation.

The ballistic limit velocity $V_L$ is obtained from the equations for the mechanics of perforation and for structural response [11, 13,14]. For applying the kinetic equations [11] to the present problem, a number of factors and material constants that appear in those equations are specified as follows:

K - nose shape factor, eq. (7) of [11]: taken to be 1/2 (spherical shape) for soft targets in which the plugs tear out and mold to the projectile (e.g. 1100-H16 Al), and unity for hard targets that flatten projectile and in which the plugs form by shearing action (e.g. 6061-T6 Al); K = 1/2 for the first layer since initial projectile shape is approximately spherical.

$A_i, D_i$ - area and diameter of cavity for the different stages of perforation according to [11]: taken to be constant over each individual, relatively thin, layer thickness with the experimentally observed average value of each layer used in the calculations ($D_i$ same as d in eqs. (1) and (2)).

e - width of shear zone: values obtained from [12] for corresponding material.

b - plug length: taken from results of [12] for corresponding material and thickness. (Note: $b \neq h$ in calculation of $V_L$ although $b = h$ is used as an approximation in the energy balance eqs. (1) and (2)).

$\mu$ - coefficient of viscosity in rate equation (15) of [11] for shear strength: taken to have value specified in [12] for similar material.

$\sigma_c, \tau_0, \gamma_f$ - material properties: compressive and shear strengths and failure shear strain as defined and used in [11] - measured for specimens used in experiments. (Note: no strain rate factors were applied to $\sigma_c$ and $\gamma_f$ in this investigation.)

Values of these material parameters for the projectile and target plates used in the associated experimental program are listed in Table 1. With these factors and material constants, the kinetic equations of [11] enable determination of $V_f$ and $t_f$, the final velocity and the perforation time, for a prescribed $V_i$. These results are then used in a computational algorithm together with structural

response results to obtain $V_L$, i.e. the $V_i$ for which $V_f = V_s$ (the structural velocity when $t = t_f$). This redefinition of $V_L$ states that the threshhold of perforation is the physical situation when the projectile velocity after penetrating a distance equal to the layer thickness is equal to the structural velocity at that point.

In the case of beam targets, we used Parkes' analyses [13,14] for the time dependent response of a rigid-plastic, clamped end beam with no axial restraint subjected to the impact of a mass that remains in contact with the beam. Each layer of the target, whether separated or in contact, is considered an independent beam in this calculation. For the case of beams in contact, the interaction effect between layers is considered in the compressive energy term in eq. (2) which is a more convenient procedure than calculating $V_L$ for the multiple layers. According to the rigid-plastic beam model, the initial stage of motion is a lateral deformation at the point of impact and the movement of a symmetrical pair of plastic hinges away from that point.

The structural velocity $V_s$ at the impact point of a beam struck by a mass $m_i$ with velocity $V_i$ is given by eq. (5) of [14] as

$$V_s = V_i/[1 + (\rho hwz/m_i)] \qquad (3)$$

where $\rho$ is the beam density, h its thickness, w its width and z the distance traveled by the plastic hinge from the impact point. The distance z is a function of time after impact, t, and can be obtained by inverting eq. (4) of [14],

$$z = \frac{6Mt}{m_i V_i} + \frac{1}{2}\left[\left(\frac{12Mt}{V_i m_i}\right)^2 + \frac{48Mt}{\rho h w V_i}\right]^{1/2} \qquad (4)$$

where M is the plastic limit moment ($M = \sigma_y wh^2/4$) and $\sigma_y$ is the dynamic yield stress. In this application, the beam response could be well approximated by a constant value of $\sigma_y$ determined by a strain rate factor on the "static" yield stress, e.g. [15]. Various experimental results, e.g. [16], indicate that a rate factor of 1.3 is reasonable for the dynamic plastic response of clamped aluminum alloy beams.

To obtain $V_L$ for a beam of a given material and dimensions impacted by a projectile of known mass and diameter, a trial and error procedure is employed to determine $V_i$ (= $V_L$) for which $V_f = V_s$ at $t = t_f$ where $V_f$ is the final velocity according to [11]. Then when $V_i > V_L$, the residual velocity $V_r$ for each layer of the target is computed from eq. (1) or (2) on a sequential basis and applied as $V_i$ to the following layer. The projectile will be stopped when $V_r < V_L$ for the next layer. It is noted that $V_L$ generally increases with each layer because of the increase of d with penetration distance.

The permanent deformation of each of the layers could be calculated from the equations of [14] noting that the projectile mass remains in contact with the beam only during the perforation time. For mid-span impact on the layer that stops the projectile, the permanent central deformation is obtained from [14] as

$$y_c = \frac{m_i^2 V_i^2}{24\rho whM}\left[\frac{\beta + 2(1+\beta)\ell n(1+\beta)}{(1+\beta)}\right] \qquad (5)$$

where $\beta = \rho whL/2m_i$ and L is the beam length. Eq. (5) would apply for a separate layer, but unperforated layers in contact would bend together without shear interactions for large plastic deformations. Eq. (5) would also be applicable for this case with h and M multiplied by the number of layers forward of the stopped projectile.

## Experiments

A number of tests were performed in an instrumented ballistic range on multi-layered targets composed of sets of aluminum beams (strips of thin plating) which were either all in contact or uniformly separated. The individual strip thicknesses were all identical in a particular target but were not the same for different targets, and the number of layers varied from one to the number needed to stop the projectile. The specimen materials were commercially pure aluminum (1100-H16) and alloy 6061-T6; thicknesses and material properties are given in Table 1. Sheets of 1100 aluminum of 1mm thickness were only available in the 1100-H14 form. The projectile was a standard 0.22 in. caliber lead bullet with an average velocity of 375 m/sec. Properties of the projectile are also listed in Table 1.

The beam specimens were 40mm wide with 230mm of free length. They were firmly clamped at their ends in a manner that was intended to permit axial movement. Spacing for the separated layers was about 13mm which was adequate to prevent interactions.

The ballistic range and its basic instrumentation was the same as that described in [12] and [17]. A pair of photocells and a counter measured the initial impact velocity while a third photocell in line activated a pulse generator through a set of time delay units. These were used to generate stroboscopic flashes at specified intervals to take a triple exposure photograph of the projectile after it perforated the target. A schematic of the

arrangement is shown in Fig. 1. Calibration of the scale of the photograph was made from a triple exposure photograph of an unimpeded bullet of measured velocity. In each test, the final velocity $V_r$ was determined by the positions of three images of the projectile on the photograph. Total perforation time of the target could be obtained by the delay time from the trigger (third) photocell to the first flash knowing the distance of that photocell to the front surface of the specimen, the distance from the rear surface to the projectile at the flash instant, and $V_i$ and $V_r$. The actual time for perforation of the beams constituting the spaced targets could be obtained by subtracting the free flight times between layers which would be known from previous tests in the series.

A test series of a given target material, beam thickness, and configuration consisted of adding layers one at a time with each test until the 0.22 in. caliber bullet was stopped. Examples of these tests are shown in the triple exposure flash photographs of Figs. 2, 3, and 4.

## Discussion of Results

Figure 2 shows a series of tests on 1100-H14 aluminum beams of 1mm thickness spaced 13mm apart. The time interval between the exposures varied from 74 μs to 112 μs. Points of interest on the photographs are that shearing of the plug is accompanied by tearing, and the ejected material molds to the projectile and travels with it as a unit with a spherical nose; the projectile path remains essentially straight; the cavity diameter increases with penetration distance in a nonlinear manner; structural motion is insignificant and limited to the perforation region until the projectile velocity decreases and approaches the ballistic limit of an individual layer. For the system shown in Fig. 2, 10 layers were required to stop the bullet and the final two beams showed large plastic deformation.

In Fig. 3, the beam specimens were of 6061-T6 aluminum and were also 1mm thick. As in the previous case, the plugs joined the bullet traveling with it as a unit along a straight path. For this harder target material, the plugs were ejected primarily by shearing action with relatively little tearing which resulted in a flat nose for the composite projectile. The time interval between exposures was 100 μs in these photographs; structural motion during the perforation times could be observed when the impact velocity is close to the ballistic limit. Nonlinear cavity growth with penetration distance is also observed. Results similar to Figs. 2 and 3 were obtained for the various tests on spaced targets using different

thicknesses of the two specimen materials.

A typical example of the response of target beams in contact is shown in Fig. 4 for 1mm thick 1100-H14 aluminum layers. When the total thickness $h_T$ is small, the impact velocities are much higher than $V_L$ and the structural deformation is minor and limited to the perforation zone. The composite projectile moves in a straight path in this case as well and acquires a rounded nose since the ejected soft target material molds to the bullet. As the number of layers approaches the ballistic limit condition, the beams divide into an initial group that experiences minor structural deformation and a downstream group (usually 2 or 3 in number) that deform together. Addition of layers near the limiting condition generally causes the bullet to appreciably slow down or stop at a lower penetration depth due to the higher compressive force. This leads to the downstream layers experiencing a high impulse and therefore large plastic deformation. The associated calculation procedure accounts for these effects since the compressive force term in eq. (2) applies up to the next to last layer and the overall plastic deformation, eq. (5), depends directly on the square of the applied impulse.

A test observation was that the cavity growth with penetration distance was generally greater for layers in contact than for comparable spaced beams. The variation of cavity diameter with penetration distance is shown in Fig. 5 for 1 and 2mm 1100-H14, -H16 beams for the two geometrical conditions.

Experimental measurements in each test consisted of the exact initial velocity (which averaged 375 m/s with a maximum variation about 15 m/s), the residual velocity, the time for perforation, the

cavity diameters for each beam, the maximum permanent deflection of each beam, and the masses of the projectile and ejected material after perforation. Details of the experimental results and corresponding theoretical predictions based on the proposed analytical procedure are given in Tables 2 and 3 and in [19]. The calculations utilized the measured cavity diameters and the material properties listed in Table 1, but were otherwise independent of empirical factors. Theoretical perforation times were not computed although it is possible to obtain approximate values for them from the equations of [11]. Measured contact times for perforation varied with total target thickness and were relatively independent of individual layer thicknesses. Comparison of the measured and calculated structural deformations show a large amount of scatter but with a number of cases of very good agreement. The observed deformation values are almost always less than the predictions which is probably due to some axial restraint in the target beams and the neglect of strain hardening in the analysis. The large scatter of structural deformation results could be due to the relatively wide width of the experimental beams, the neglect of the penetration energy in eq. (5), and also to the sensitivity of the system to small variations of the governing parameters near the ballistic limit condition.

A reasonable basis to compare the experimental results with the proposed analytical procedure is to examine the dependence of the parameter $\Delta V/V_i$ (where $\Delta V$ is the velocity drop) on the total target thickness. This is a fairly standard method for representing ballistic test results [2]. A number of examples of experimental

and associated analytical results are shown in Figs. 6 to 10.

An overall comparison of these results indicates that the proposed analytical procedure does lead to reasonably good predictions. Calculated results for monolithic beam targets, Fig. 6, are in better agreement with tests than those calculated from the equations of [11] due to the inclusion of structural deformation in the present analysis. The influence of structural deformation on the perforation process could be seen by the variation of results for different individual beam thicknesses. Spaced targets become less effective as the individual layers become thinner and an optimum layer thickness appears to be about $h \sim (1/3) h_T$, Figs. 7 and 9. As expected, the stronger target material, 6061-T6, is more effective but not in proportion to its relative strength in this case. The spaced targets are generally less effective than corresponding monolithic targets although the resistance is almost the same for the optimum layer thickness. This implies that under these circumstances the effect of structural bending almost compensates for the lower shear and compressive strength of separated layers.

Layered beams in contact, Figs. 8 and 10, have the highest ballistic resistance of the systems examined as they demonstrate both compressive strength and structural deformation. In this case, the higher strength of the 6061-T6 material is more fully utilized and this material is almost twice as effective as 1100-H16 for the

optimum layer thickness condition. The ballistic resistance of laminated beams is less sensitive than spaced layers to the thickness of the individual layers, although a lamina thickness of about a third the total also appears to be optimum for this case. With this optimum lamina thickness, laminated 6061-T6 beams are about 50% more effective (i.e. require about 2/3 the weight), and 1100-H16 beams are about 25% more effective (i.e. require about 80% the weight), than monolithic targets of corresponding material.

## Conclusions

A method has been developed for including the effect of overall structural deformation in an analysis of the ballistic perforation process. Calculated results for the projectile velocity drop based on this combined theory are in fairly good agreement with corresponding experiments. A factor in the equations is the perforated cavity diameter which was obtained from the experiments. The theory is otherwise essentially self-contained within the assumptions of the analyses on which it is based. When the proposed theory is applied to multi-layered target beams, some of the consequences which are supported by the experimental data are as follows:

1. For the test conditions and specimens, the general order of ballistic resistance of the beam targets, starting with maximum, was: multi-layered flat beams in contact, an equivalent weight uniform beam, and separated flat beams of equal weight. Results for layers in contact are not very sensitive to tne thickness of the individual layer although a particular layer thickness, $h \sim (1/3)h_T$, leads to maximum ballistic resistance. Separated layers showed decreasing resistance as the individual layers became thinner. A similar optimum thickness, $h \sim (1/3)h_T$, also appears to exist for spaced targets which leads to ballistic resistance values comparable to those of a monolithic target. The relatively greater resistance of layered beams in contact is apparently due to structural deformation acting as an effective energy absorbing mechanism.

Separated layers have the least resistance in this application due to the absence of the compressive stress effect and their independence in structural deformation.

2. Consideration of structural deformation in the perforation analysis increases the ballistic limit $V_L$. On the basis of only structural motion, the ballistic limit would increase with decreasing plastic limit moment and decreasing density of the target material. These properties also have a direct effect on the perforation process so their net influence on $V_L$ is complicated.

3. Maximum structural deformation of an individual layer occurs at or close to its ballistic limit. This agrees with the observations of other investigators [9,18].

## References

1. Riney, T.D. and Halda, E.J., "Effectiveness of Meteoroid Bumpers Composed of Two Layers of Distinct Materials," AIAA Journal, vol. 6, 1968, pp. 338-344.

2. Backman, M.E. and Goldsmith, W., "The Mechanics of Penetration of Projectiles into Targets," Inter. Journal of Engineering Science, vol. 16, 1978, pp. 1-99.

3. Kreyenhagen, K.N., Wagner, M.H., Piechocki, J.J., and Bjork, R.L., "Ballistic Limit Determination in Impacts on Multi-material Laminated Targets," AIAA Journal, vol. 8, 1970, pp. 2147-2151.

4. Flaherty, R.E., "A Study of Low Velocity Impacts into Thin Sheet Aluminum and Nylon Cloth," NASA Technical Note (TN) D-6324, May 1971.

5. Zaid, A.I.O. and Travis, F.W., "A Comparison of Single and Multi-Plate Shields Subjected to Impact by a High Speed Projectile," Conf. on Mechanical Properties at High Rates of Strain, J. Harding, ed., Confer. Series No. 21, Institute of Physics, London, 1974, pp. 417-428.

6. Calder, C.A. and Goldsmith, W., "Plastic Deformation and Perforation of Thin Plates Resulting from Projectile Impact," Inter. Journal of Solids and Structures, vol. 7, 1971, pp. 863-881.

7. Beynet, P. and Plunkett, R., "Plate Impact and Plastic Deformation by Projectiles," Experimental Mechanics, vol. 11, 1971, pp. 64-70.

8. Dienes, J.K. and Miles, J.W., "A Membrane Model for the Response of Thin Plates to Ballistic Impact," Journal Mechanics and Physics of Solids, vol. 25, 1977, pp. 237-256.

9. Lethaby, J.W. and Skidmore, I.C., "The Deformation and Plugging of Thin Plates by Projectile Impact," Confer. on Mechanical Properties at High Rates of Strain, J. Harding, ed., Confer. Series No. 21, Institute of Physics, London, 1974, pp. 429-441.

10. Recht, R.F. and Ipson, T.W., "Ballistic Perforation Dynamics," Journal Applied Mechanics, vol. 30, 1963, pp. 384-390.

11. Awerbuch, J. and Bodner, S.R., "Analysis of the Mechanics of Perforation of Projectiles in Metallic Plates," Inter. Journal of Solids and Structures, vol. 10, 1974, pp. 671-684.

12. Awerbuch, J. and Bodner, S.R., "Experimental Investigation of Normal Perforation of Projectiles in Metallic Plates," Inter. Journal of Solids and Structures, vol. 10, 1974, pp. 685-699.

13. Parkes, E.W., "The Permanent Deformation of a Cantilever Struck Transversely at its Tip," Proc. Royal Soc., A., vol. 228, 1955, pp. 462-476.

14. Parkes, E.W., "The Permanent Deformation of an Encastre Beam Struck Transversely at any Point in its Span," Proc. of the Institution of Civil Engineers, vol. 10, 1958, pp. 277-304.

15. Furman, H. and Bodner, S.R., "Permanent Deformation of Clamped Beams Subjected to Oblique Impact Loading," Israel Journal of Technology, vol. 12, 1974, pp. 117-124.

16. Bodner, S.R. and Speirs, W.G., "Dynamic Plasticity Experiments on Aluminum Cantilever Beams at Elevated Temperature," Journal Mechanics and Physics Solids, vol. 11, 1963, pp. 65-77.

17. Awerbuch, J. and Bodner, S.R., "An Investigation of Oblique Perforation of Metallic Plates by Projectiles," Experimental Mechanics, vol. 17, 1977, pp. 147-153.

18. Goldsmith, W. and Finnegan, S.A., "Penetration and Perforation Processes in Metal Targets At and Above Ballistic Velocities," Inter. Journal Mechanical Sciences, vol. 13, 1971, pp. 843-866.

19. Mermelstein (Marom), I., "Projectile Penetration in Metallic Layered Targets," M.Sc. thesis, Technion - Israel Institute of Technology, Haifa, 1977.

## List of Captions

Table 1 - Properties of Target Specimens and Projectile

Table 2 - Summary of Experimental Results

Table 3 - Summary of Theoretical Results

Fig. 1 - Schematic of the experimental arrangement.

Fig. 2 - Triple exposure photographs of 0.22 in. caliber lead bullets and plugs after perforation of spaced 1100-H14 aluminum, 1mm thick target beams.

Fig. 3 - Triple exposure photographs of 0.22 in. caliber lead bullets and plugs after perforation of spaced 6061-T6 aluminum, 1mm thick target beams.

Fig. 4 - Triple exposure photographs of 0.22 in. caliber lead bullets and plugs after perforation of 1100-H14 aluminum, 1mm thick target beams in contact.

Fig. 5 - Experimental results for the cavity diameters formed by 0.22 in. caliber lead bullets perforating spaced and laminated beam targets of aluminum as a function of total material thickness.

Fig. 6 - Velocity drop as a function of target thickness of 0.22 in. caliber lead bullets perforating single beams of commercially pure and alloy aluminum (width: 40 mm; length: 230 mm).

Fig. 7 - Velocity drop as a function of total material thickness of 0.22 in. caliber lead bullets perforating spaced 1100 aluminum beams (width: 40mm; length: 230mm).

Fig. 8 - Velocity drop as a function of total material thickness of 0.22 in. caliber lead bullets perforating 1100 aluminum beams in contact (width: 40mm; length 230mm).

Fig. 9 - Velocity drop as a function of total material thickness of 0.22 in. caliber lead bullets perforating spaced aluminum alloy beams (width: 40mm; length: 230mm).

Fig. 10 - Velocity drop as a function of total material thickness of 0.22 in. caliber lead bullets perforating aluminum alloy beams in contact (width: 40mm; length 230mm).

TABLE 1 - Properties of Target Specimens and Projectile

1. Projectile

Material: lead; diameter: 0.22 in. (5.56mm); initial weight: 2.6 $gm^f$.

Average velocity at impact: 375 m/sec.

Nose factor K = 1/2 for initial impact condition.

2. Target Specimens

| Specimen Material | Layer Thickness h (mm) | Yield Strength $\sigma_y$ (static) ($kg^f/mm^2$) | Compressive Strength $\sigma_c$ ($kg^f/mm^2$) | Shear Strength $\tau_0$ (static) ($kg^f/mm^2$) | Plug Length b [12] (mm) |
|---|---|---|---|---|---|
| Al 1100-H14 | 1.0 | 12.5 | 13.5 | 7.7 | 0.7 |
| Al 1100-H16 | 2.0 | 14 | 16.5 | 8.4 | 1.4 |
| Al 1100-H16 | 2.5 | 14 | 16.5 | 8.4 | 1.7 |
| Al 1100-H16 | 3.0 | 14 | 16.5 | 8.4 | 2.2 |
| Al 6061-T6 | 1.0 | 24 | 28 | 21.1 | 0.65 |
| Al 6061-T6 | 1.7 | 24 | 28 | 21.1 | 1.2 |
| Al 6061-T6 | 2.1 | 28 | 33.2 | 21.1 | 1.5 |
| Al 6061-T6 | 3.6 | 26 | 31.5 | 21.1 | 2.5 |
| Al 6061-T6 | 4.76 | 28 | 34.6 | 21.1 | - |

weight density: 2.7 $gm^f/cm^3$

width of shear zone e, [12]: Al 1100: 1.3mm; Al 6061: 1.5mm

shear strength rate coeff. $\mu$, [12]: Al 1100: ?; Al 6061: 10 ($gm.sec/cm^2$)

strain rate factor on $\sigma_y$: Al 1100: 1.3; Al 6061: 1.3

Failure strain in shear $\gamma_f$ [12]: 0.20

## Table 2 - Summary of Experimental Results

(a) Target Material: 1100-H14 Aluminum; Layer Thickness: h.
Beam Width: 40 mm.; Beam Length: 230 mm.

| h (mm) | Number of Layers | Layer Spacing (mm) | Initial Velocity (m/sec) | Final Velocity (m/sec) | Contact Duration (μsec) | Cavity Diameter (mm) Layer No. 1 | 2 | 3 | 4 | 5 | 6 | 7 | 8 | 9 | 10 | Maximum Deflection (at center) (mm) Layer No. 1 | 2 | 3 | 4 | 5 | 6 | 7 | 8 | 9 | 10 |
|---|---|---|---|---|---|---|---|---|---|---|---|---|---|---|---|---|---|---|---|---|---|---|---|---|---|
| 1 | 1 | 0 | 387 | 369 | 5.1 | 5.9 | | | | | | | | | | 0.7 | | | | | | | | | |
| 1 | 2 | 13 | 374 | 344 | 13 | 5.9 | 6.5 | | | | | | | | | 0.7 | 0.8 | | | | | | | | |
| 1 | 3 | 13 | 374 | 326 | 19.5 | 5.9 | 6.5 | 7.6 | | | | | | | | 0.7 | 0.8 | 0.9 | | | | | | | |
| 1 | 4 | 13 | 377 | 318 | 40 | 5.9 | 6.5 | 7.6 | 8.3 | | | | | | | 0.7 | 0.8 | 0.9 | 1.0 | | | | | | |
| 1 | 5 | 13 | 373 | 284 | 64 | 5.9 | 6.5 | 7.6 | 8.3 | 8.4 | | | | | | 0.7 | 0.8 | 0.9 | 1.0 | 1.5 | | | | | |
| 1 | 6 | 13 | 380 | 249 | 76 | 5.9 | 6.5 | 7.6 | 8.3 | 8.4 | 8.6 | | | | | 0.7 | 0.8 | 0.9 | 1.0 | 1.5 | 1.9 | | | | |
| 1 | 7 | 13 | 376 | 236 | 106 | 5.9 | 6.5 | 7.6 | 8.3 | 8.4 | 8.6 | 8.7 | | | | 0.7 | 0.8 | 0.9 | 1.0 | 1.5 | 1.9 | 2.8 | | | |
| 1 | 8 | 13 | 377 | 207 | 137 | 5.9 | 6.5 | 7.6 | 8.3 | 8.4 | 8.6 | 8.7 | 9.0 | | | 0.7 | 0.8 | 0.9 | 1.0 | 1.5 | 1.9 | 2.8 | 4.0 | | |
| 1 | 9 | 13 | 375 | 139 | 156 | 5.9 | 6.5 | 7.6 | 8.3 | 8.4 | 8.6 | 8.7 | 9.0 | 10 | 0 | 0.7 | 0.8 | 0.9 | 1.0 | 1.5 | 1.9 | 2.8 | 4.0 | 12 | |
| 1 | 10 | 13 | 376 | 0 | ∞ | 5.9 | 6.5 | 7.6 | 8.3 | 8.4 | 8.6 | 8.7 | 9.0 | 10 | 0 | 0.7 | 0.8 | 0.9 | 1.0 | 1.5 | 1.9 | 2.8 | 4.0 | 12 | 12.2 |
| 1 | 2 | 0 | 385 | 356 | 10 | 6.2 | 6.5 | | | | | | | | | 0.2 | 1.0 | | | | | | | | |
| 1 | 3 | 0 | 362 | 297 | 26 | 6.2 | 7.8 | 8.5 | | | | | | | | 1.5 | 2.0 | 2.5 | | | | | | | |
| 1 | 4 | 0 | 369 | 267 | 44 | 6.3 | 8.2 | 8.9 | 8.9 | | | | | | | 1.1 | 2.4 | 3.5 | 3.5 | | | | | | |
| 1 | 5 | 0 | 367 | 190 | 72 | 6.4 | 8.3 | 9.3 | 9.3 | 9.1 | | | | | | 1.0 | 2.2 | 5.4 | 8.3 | 8.3 | | | | | |
| 1 | 6 | 0 | 359 | 115 | 135 | 6.6 | 8.5 | 8.8 | 8.3 | 7.7 | 7.7 | | | | | 1.1 | 2.0 | 7.8 | 1.0 | 12 | 12 | | | | |
| 1 | 7 | 0 | 366 | 0 | ∞ | 6.7 | 9.0 | 9.0 | | | | | | | | 1.0 | 2.5 | 9.7 | 9.7 | 9.7 | 9.7 | 9.7 | | | |

Table 2 - Summary of Experimental Results (cont'd)

(b) Target Material: 1100-H16 Aluminum; Layer Thickness: h.
Beam Width: 40 mm., Beam Length: 230 mm.

| h (mm) | Number of Layers | Layer Spacing (mm) | Initial Velocity (m/sec) | Final Velocity (m/sec) | Contact Duration (μsec) | Cavity Diameter (mm) Layer No. | | | | | | | | | | Maximum Deflection (at center) (mm) Layer No. | | | | | | | | | |
|---|---|---|---|---|---|---|---|---|---|---|---|---|---|---|---|---|---|---|---|---|---|---|---|---|---|
| | | | | | | 1 | 2 | 3 | 4 | 5 | 6 | 7 | 8 | 9 | 10 | 1 | 2 | 3 | 4 | 5 | 6 | 7 | 8 | 9 | 10 |
| 2 | 1 | 0 | 385 | 346 | 10 | 6.0 | | | | | | | | | | 1.4 | | | | | | | | | |
| 2 | 2 | 13 | 383 | 280 | 47 | 6.0 | 7.1 | | | | | | | | | 1.4 | 3.4 | | | | | | | | |
| 2 | 3 | 13 | 370 | 153 | 107 | 6.0 | 7.1 | 10 | | | | | | | | 1.4 | 3.4 | 8.9 | | | | | | | |
| 2 | 4 | 13 | 375 | 0 | ∞ | 6.0 | 7.1 | 10 | 0 | | | | | | | 1.4 | 3.4 | 8.9 | 7.9 | | | | | | |
| 2 | 2 | 0 | 369 | 256 | 42 | 6.6 | 8.4 | | | | | | | | | 1.1 | 3.6 | | | | | | | | |
| 2 | 3 | 0 | 377 | 45 | 176 | 7.0 | 8.8 | 8.8 | | | | | | | | 1.5 | 9.2 | 11 | | | | | | | |
| 2.5 | 1 | 0 | 381 | 341 | 13 | 6.0 | | | | | | | | | | 2.1 | | | | | | | | | |
| 2.5 | 2 | 13 | 369 | 225 | 78 | 6.0 | 8.8 | | | | | | | | | 2.1 | 4.6 | | | | | | | | |
| 2.5 | 3 | 13 | 376 | 0 | ∞ | 6.0 | 8.8 | 0 | | | | | | | | 2.1 | 4.6 | 13 | | | | | | | |
| 2.5 | 2 | 0 | 379 | 241 | 62 | 6.8 | 8.4 | | | | | | | | | 1.4 | 5.5 | | | | | | | | |
| 2.5 | 3 | 0 | 375 | 0 | ∞ | 7.2 | 0 | 0 | | | | | | | | 1.2 | 8.7 | 9.0 | | | | | | | |
| 3 | 1 | 0 | 397 | 332 | 15 | 6.3 | | | | | | | | | | 1.2 | | | | | | | | | |
| 3 | 2 | 13 | 371 | 120 | 140 | 6.3 | 9.6 | | | | | | | | | 1.2 | 6.0 | | | | | | | | |
| 3 | 3 | 13 | 375 | 0 | ∞ | 6.3 | 9.6 | 0 | | | | | | | | 1.2 | 6.0 | 11 | | | | | | | |
| 3 | 2 | 0 | 365 | 110 | 140 | 7.2 | 1.0 | 0 | | | | | | | | 1.5 | 7.0 | | | | | | | | |
| 3 | 3 | 0 | 370 | 0 | ∞ | 7.8 | 9.0 | 0 | | | | | | | | 1.5 | 5.0 | 5.0 | | | | | | | |

## Table 2 - Summary of Experimental Results (cont'd)

(c) Target Material: 6061-T6 Aluminum; Layer Thickness: h.
Beam Width: 40 mm.; Beam Length: 230 mm.

| h (mm) | Number of Layers | Layer Spacing (mm) | Initial Velocity (m/sec) | Final Velocity (m/sec) | Contact Duration (μsec) | Cavity Diameter (mm) Layer No. | | | | | | | | | | Maximum Deflection (at center) (mm) Layer No. | | | | | | | | | |
|---|---|---|---|---|---|---|---|---|---|---|---|---|---|---|---|---|---|---|---|---|---|---|---|---|---|
| | | | | | | 1 | 2 | 3 | 4 | 5 | 6 | 7 | 8 | 9 | 10 | 1 | 2 | 3 | 4 | 5 | 6 | 7 | 8 | 9 | 10 |
| 1 | 1 | 0 | 379 | 357 | 5 | 5.7 | | | | | | | | | | 1.3 | | | | | | | | | |
| 1 | 2 | 13 | 359 | 321 | 15 | 5.7 | 6.4 | | | | | | | | | 1.3 | 1.6 | | | | | | | | |
| 1 | 3 | 13 | 357 | 302 | 19 | 5.7 | 6.4 | 7.0 | | | | | | | | 1.3 | 1.6 | 1.8 | | | | | | | |
| 1 | 4 | 13 | 368 | 294 | 43 | 5.7 | 6.4 | 7.0 | 7.3 | | | | | | | 1.3 | 1.6 | 1.8 | 1.8 | | | | | | |
| 1 | 5 | 13 | 357 | 258 | 68 | 5.7 | 6.4 | 7.0 | 7.3 | 7.4 | | | | | | 1.3 | 1.6 | 1.8 | 1.8 | 2.4 | | | | | |
| 1 | 6 | 13 | 363 | 234 | 81 | 5.7 | 6.4 | 7.0 | 7.3 | 7.4 | 7.8 | | | | | 1.3 | 1.6 | 1.8 | 1.8 | 2.4 | 2.8 | | | | |
| 1 | 7 | 13 | 368 | 201 | 135 | 5.7 | 6.4 | 7.0 | 7.3 | 7.4 | 7.8 | 7.8 | | | | 1.3 | 1.6 | 1.8 | 1.8 | 2.4 | 2.8 | 7.0 | | | |
| 1 | 8 | 13 | 360 | 115 | 223 | 5.7 | 6.4 | 7.0 | 7.3 | 7.4 | 7.8 | 7.8 | 7.5 | | | 1.3 | 1.6 | 1.8 | 1.3 | 2.4 | 2.8 | 7.0 | 16 | | |
| 1 | 2 | 0 | 367 | 311 | 32 | 6.9 | 6.9 | | | | | | | | | 3.1 | 4.4 | | | | | | | | |
| 1 | 3 | 0 | 355 | 230 | 87 | 7.7 | 7.2 | 7.5 | | | | | | | | 5.5 | 5.6 | 7.0 | | | | | | | |
| 1 | 4 | 0 | 362 | 146 | 119 | 8.5 | 8.0 | 7.7 | 7.5 | | | | | | | 3.9 | 6.9 | 8.5 | 9.1 | | | | | | |
| 1 | 5 | 0 | 369 | 0 | ∞ | 7.5 | 7.6 | 0 | 0 | 0 | | | | | | 5.7 | 7.3 | 7.6 | 8.5 | 8.4 | | | | | |
| 1.7 | 1 | 0 | 378 | 332 | 13 | 6.1 | | | | | | | | | | 2.9 | | | | | | | | | |
| 1.7 | 2 | 16 | 356 | 244 | 50 | 6.1 | 7.8 | | | | | | | | | 2.9 | 3.9 | | | | | | | | |
| 1.7 | 3 | 16 | 371 | 146 | 166 | 6.1 | 7.8 | 8.8 | | | | | | | | 2.9 | 3.9 | 9.2 | | | | | | | |
| 1.7 | 2 | 0 | 370 | 0 | ∞ | 0 | 0 | | | | | | | | | 9.2 | 11 | | | | | | | | |
| 2.1 | 1 | 0 | 357 | 293 | 32 | 6.1 | | | | | | | | | | 3.6 | | | | | | | | | |
| 2.1 | 2 | 13 | 367 | 200 | 68 | 6.1 | 7.7 | | | | | | | | | 3.6 | 6.1 | | | | | | | | |
| 2.1 | 3 | 13 | 352 | 0 | ∞ | 6.1 | 7.7 | 0 | | | | | | | | 3.6 | 6.1 | 3.0 | | | | | | | |
| 2.1 | 2 | 0 | 360 | 0 | ∞ | 0 | 0 | | | | | | | | | 7.2 | 7.2 | | | | | | | | |
| 3.6 | 1 | 0 | 365 | 249 | 14 | 6.5 | | | | | | | | | | 3.6 | | | | | | | | | |
| 3.6 | 2 | 13 | 370 | 0 | ∞ | 6.5 | 0 | | | | | | | | | 3.6 | 3.3 | | | | | | | | |
| 3.6 | 2 | 0 | 368 | 0 | ∞ | 0 | 0 | | | | | | | | | 3.2 | 3.2 | | | | | | | | |

Table 3 - Summary of Theoretical Results

| Target Material | Layer Thickness (mm) | Number of Layers | Layer Spacing (mm) | Initial Velocity (m/sec) | Final Velocity (m/sec) Layer No. 1 | 2 | 3 | 4 | 5 | 6 | 7 | 8 | 9 | 10 | Maximum Deflection (mm) |
|---|---|---|---|---|---|---|---|---|---|---|---|---|---|---|---|
| 1100-H14 | 1 | 10 | ∞ | 380 | 372.7 | 361.5 | 342.9 | 316.1 | 283.7 | 247.8 | 207.0 | 158.1 | 85 | 0 | 23 |
| 1100-H14 | 1 | 6 | 0 | 375 | 345.8 | 319.2 | 282.9 | 225.2 | 145.2 | 42.6 | 0 | | | | 11 |
| 1100-H16 | 2 | 4 | ∞ | 380 | 337.6 | 272.1 | 185.8 | 0 | | | | | | | 34 |
| 1100-H16 | 2 | 3 | 0 | 375 | 303.9 | 207.1 | 0 | | | | | | | | 39 |
| 1100-H16 | 2.5 | 3 | ∞ | 380 | 326.2 | 244.8 | 0 | | | | | | | | 31 |
| 1100-H16 | 2.5 | 3 | 0 | 375 | 282.4 | 174.1 | 0 | | | | | | | | 18 |
| 1100-H16 | 3 | 3 | ∞ | 375 | 288.8 | 175.2 | 0 | | | | | | | | 13.4 |
| 1100-H16 | 3 | 3 | 0 | 375 | 264.2 | 127.7 | 0 | | | | | | | | 6.3 |
| 1100-H16 | 4 | 1 | 0 | 375 | 295.4 | | | | | | | | | | |
| 1100-H16 | 5 | 1 | 0 | 375 | 264.4 | | | | | | | | | | |
| 1100-H16 | 6 | 1 | 0 | 375 | 206 | | | | | | | | | | |
| 1100-H16 | 7 | 1 | 0 | 375 | 122.1 | | | | | | | | | | |
| 1100-H16 | 7.5 | 1 | 0 | 375 | 0 | | | | | | | | | | |

Beam Width: 40 mm.; Beam Length: 230 mm.

Table 3 - Summary of Theoretical Results (continued)

| Target Material | Layer Thickness (mm) | Number of Layers | Layer Spacing (mm) | Initial Velocity (m/sec) | Final Velocity (m/sec) Layer No. 1 | 2 | 3 | 4 | 5 | 6 | 7 | 8 | 9 | 10 | Maximum Deflection (mm) |
|---|---|---|---|---|---|---|---|---|---|---|---|---|---|---|---|
| 6061-T6 | 1 | 8 | ∞ | 375 | 351.7 | 344.1 | 325.9 | 296.7 | 254.6 | 189.0 | 38.6 | 0 | | | 16 |
| 6061-T6 | 1 | 4 | 0 | 375 | 326.7 | 260.2 | 160.7 | 0 | | | | | | | 53 |
| 6061-T6 | 1.7 | 4 | ∞ | 375 | 325.0 | 253.3 | 150.6 | 0 | | | | | | | 23 |
| 6061-T6 | 1.7 | 2 | 0 | 375 | 291.3 | 0 | | | | | | | | | 67 |
| 6061-T6 | 2.1 | 3 | ∞ | 375 | 312.8 | 206.6 | 0 | | | | | | | | 20 |
| 6061-T6 | 2.1 | 2 | 0 | 375 | 194.8 | 0 | | | | | | | | | 15.7 |
| 6061-T6 | 3.6 | 3 | ∞ | 375 | 255.8 | 25.8 | 0 | | | | | | | | 0.1 |
| 6061-T6 | 3.6 | 2 | 0 | 375 | 147.1 | 0 | | | | | | | | | 2.8 |
| 6061-T6 | 4.7 | 1 | 0 | 365 | 140.9 | | | | | | | | | | |
| 6061-T6 | 5.5 | 1 | 0 | 365 | 95.9 | | | | | | | | | | |
| 6061-T6 | 6 | 1 | 0 | 375 | 0 | | | | | | | | | | |

Beam Width: 40 mm.; Beam Length: 230 mm.

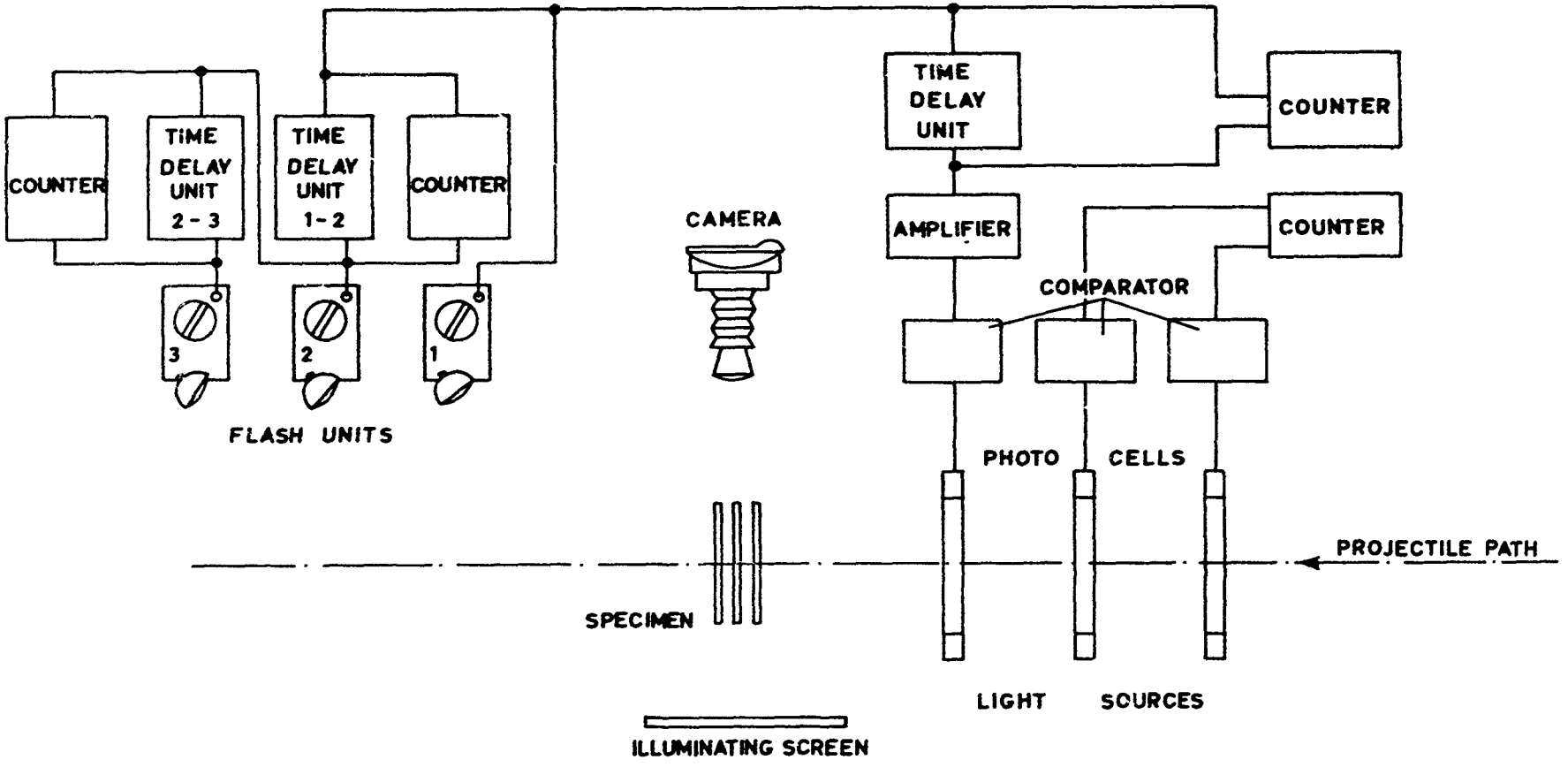
COUNTER
TIME DELAY UNIT 2 - 3
TIME DELAY UNIT 1 - 2
COUNTER
3
2
1
FLASH UNITS
CAMERA
TIME DELAY UNIT
COUNTER
AMPLIFIER
COUNTER
COMPARATOR
PHOTO CELLS
PROJECTILE PATH
SPECIMEN
LIGHT SOURCES
ILLUMINATING SCREEN

FIG. 1

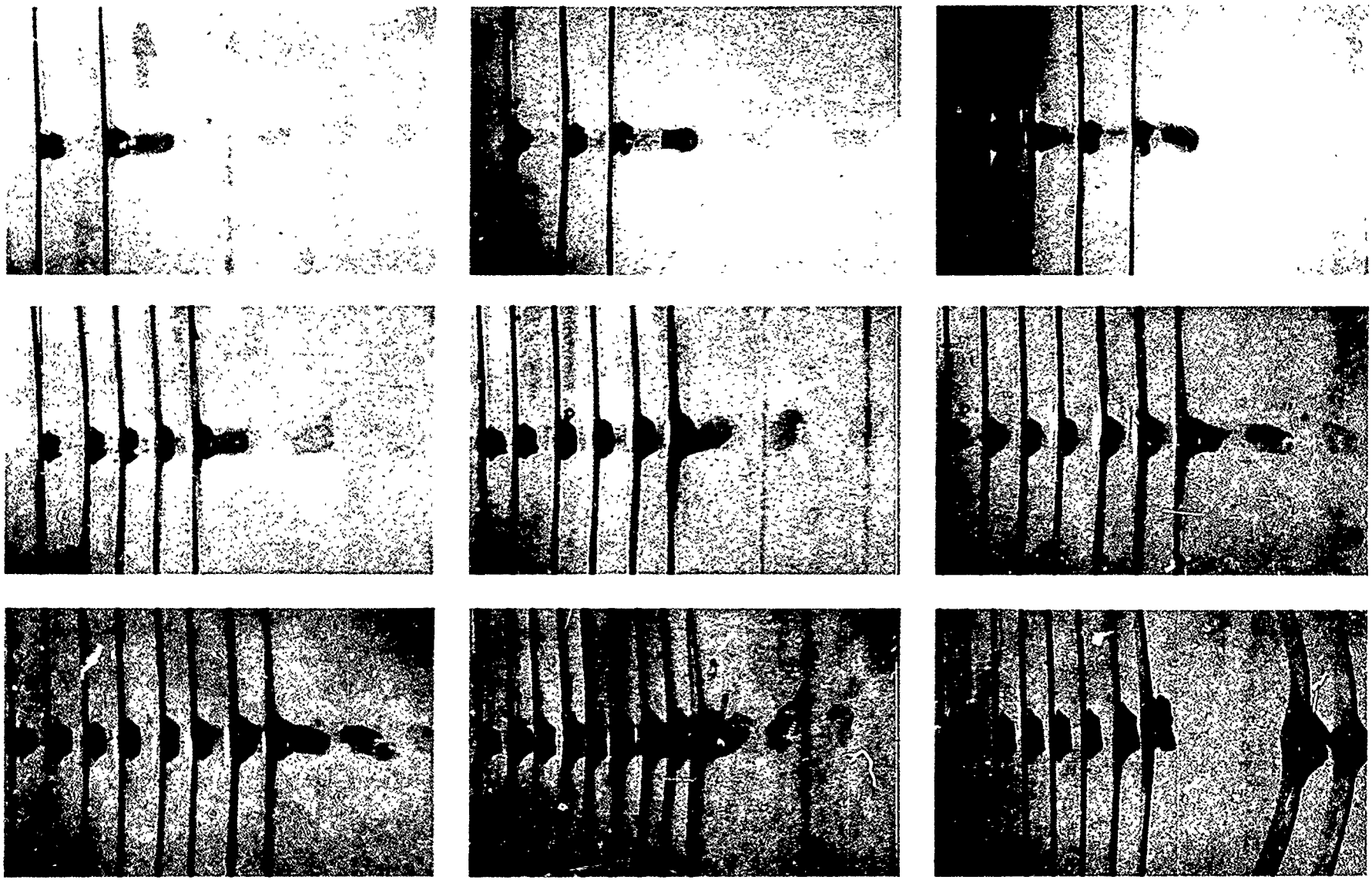

FIG. 2

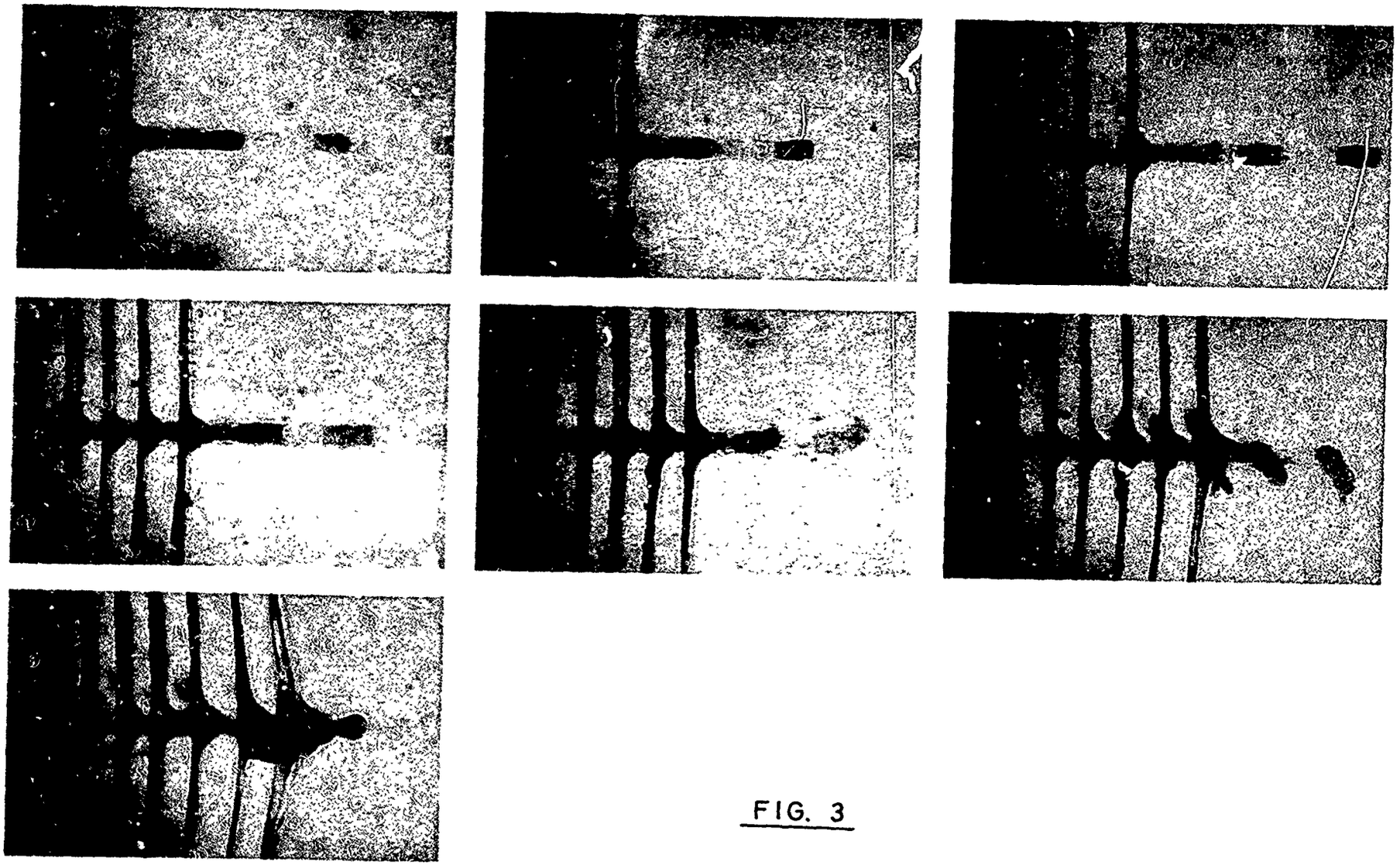

FIG. 3

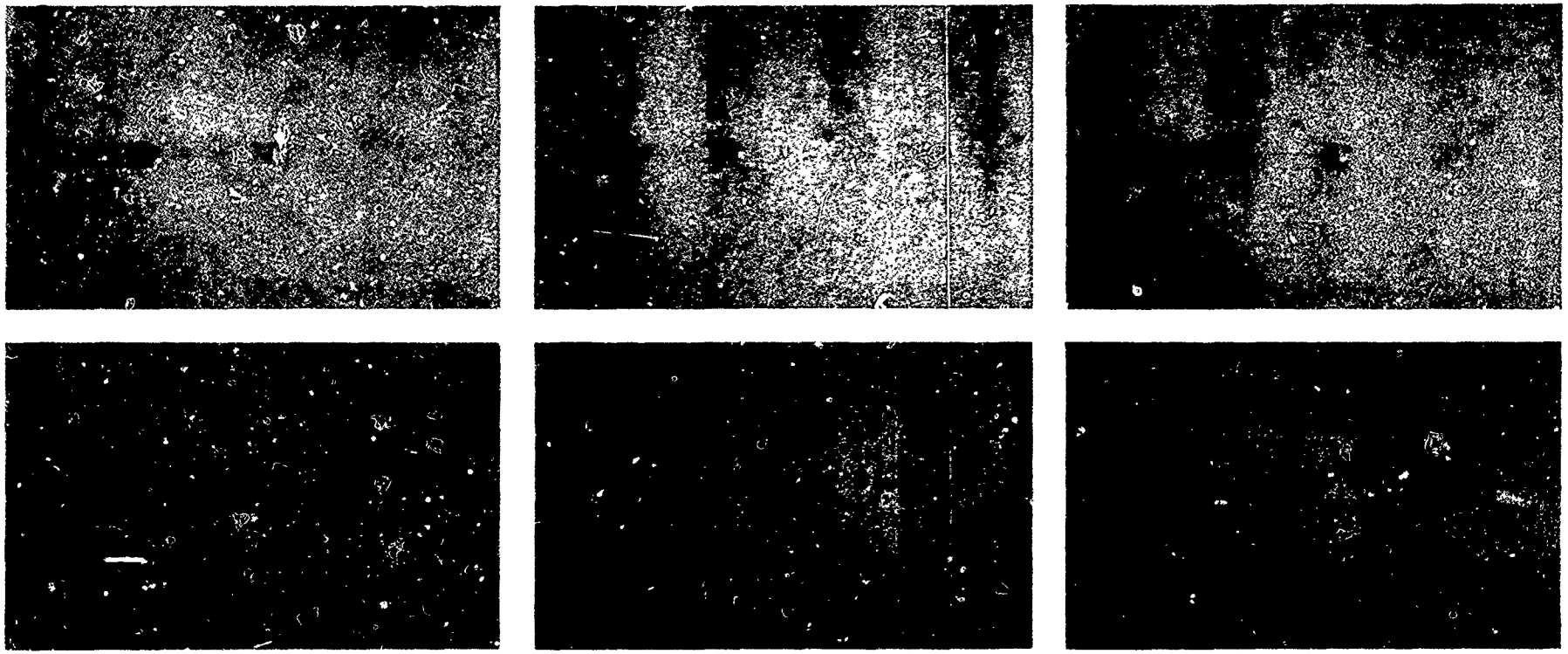

FIG. 4

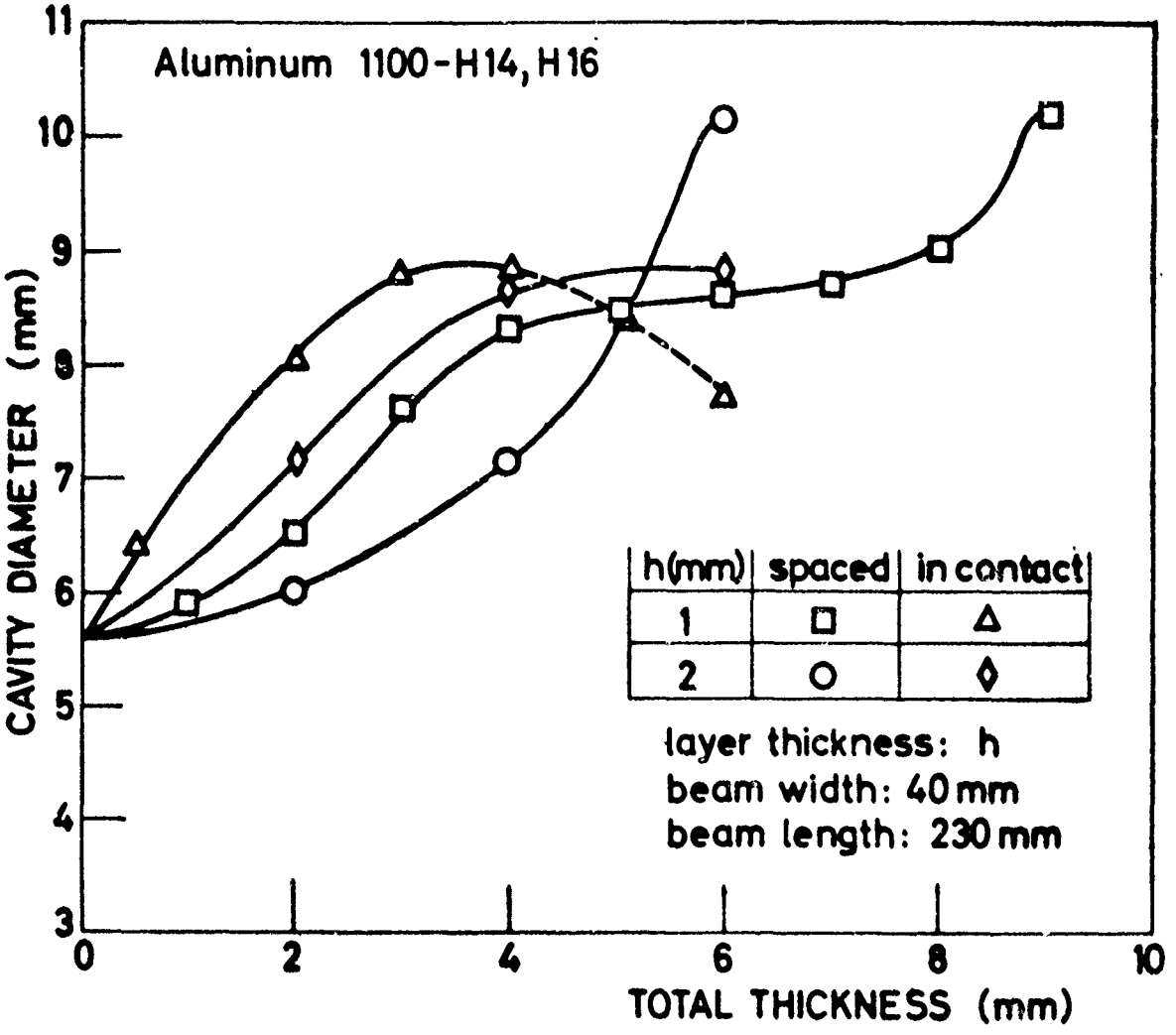
Aluminum 1100-H14, H16
CAVITY DIAMETER (mm)
TOTAL THICKNESS (mm)
11
10
9
8
7
6
5
4
3
0
2
4
6
8
10
h(mm) | spaced | in contact
1 | □ | △
2 | ○ | ◊
layer thickness: h
beam width: 40 mm
beam length: 230 mm

FIG. 5

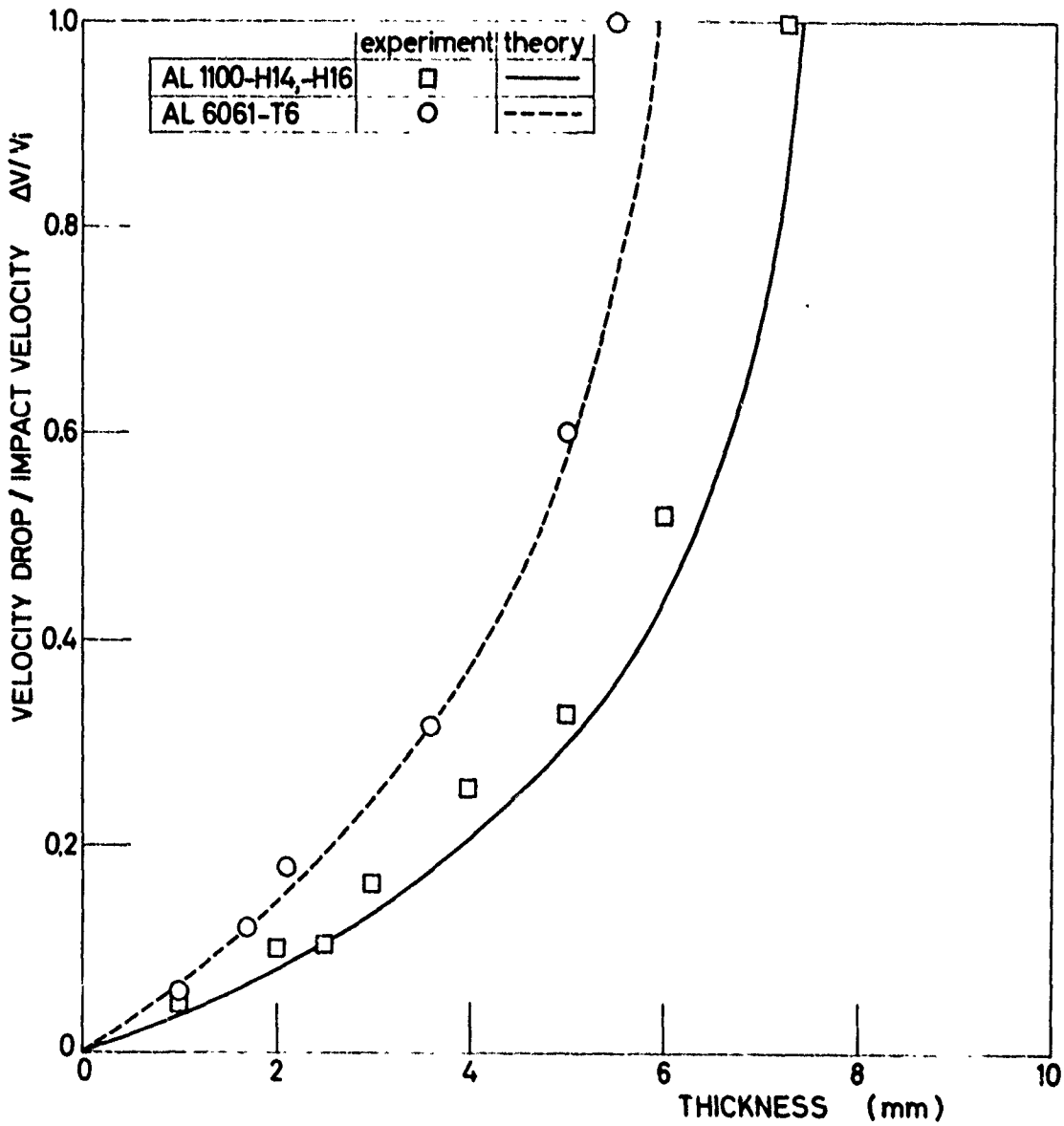
experiment
theory
AL 1100-H14,-H16
AL 6061-T6
VELOCITY DROP / IMPACT VELOCITY ΔV/Vi
1.0
0.8
0.6
0.4
0.2
0
0
2
4
6
8
10
THICKNESS (mm)

FIG. 6

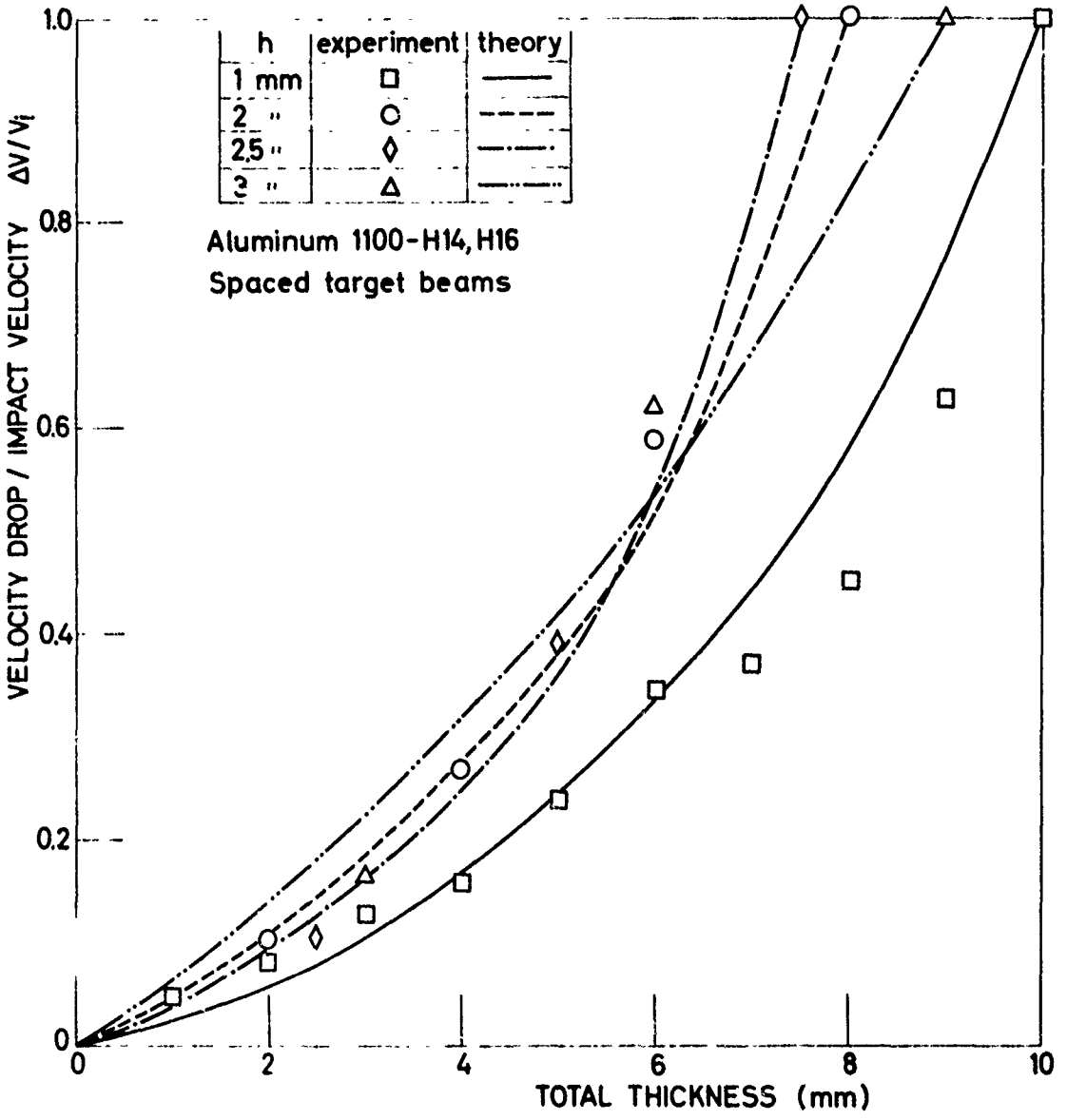
h
experiment
theory
1 mm
2 "
2.5 "
3 "
Aluminum 1100-H14, H16
Spaced target beams
VELOCITY DROP / IMPACT VELOCITY ΔV/Vi
1.0
0.8
0.6
0.4
0.2
0
0
2
4
6
8
10
TOTAL THICKNESS (mm)

FIG. 7

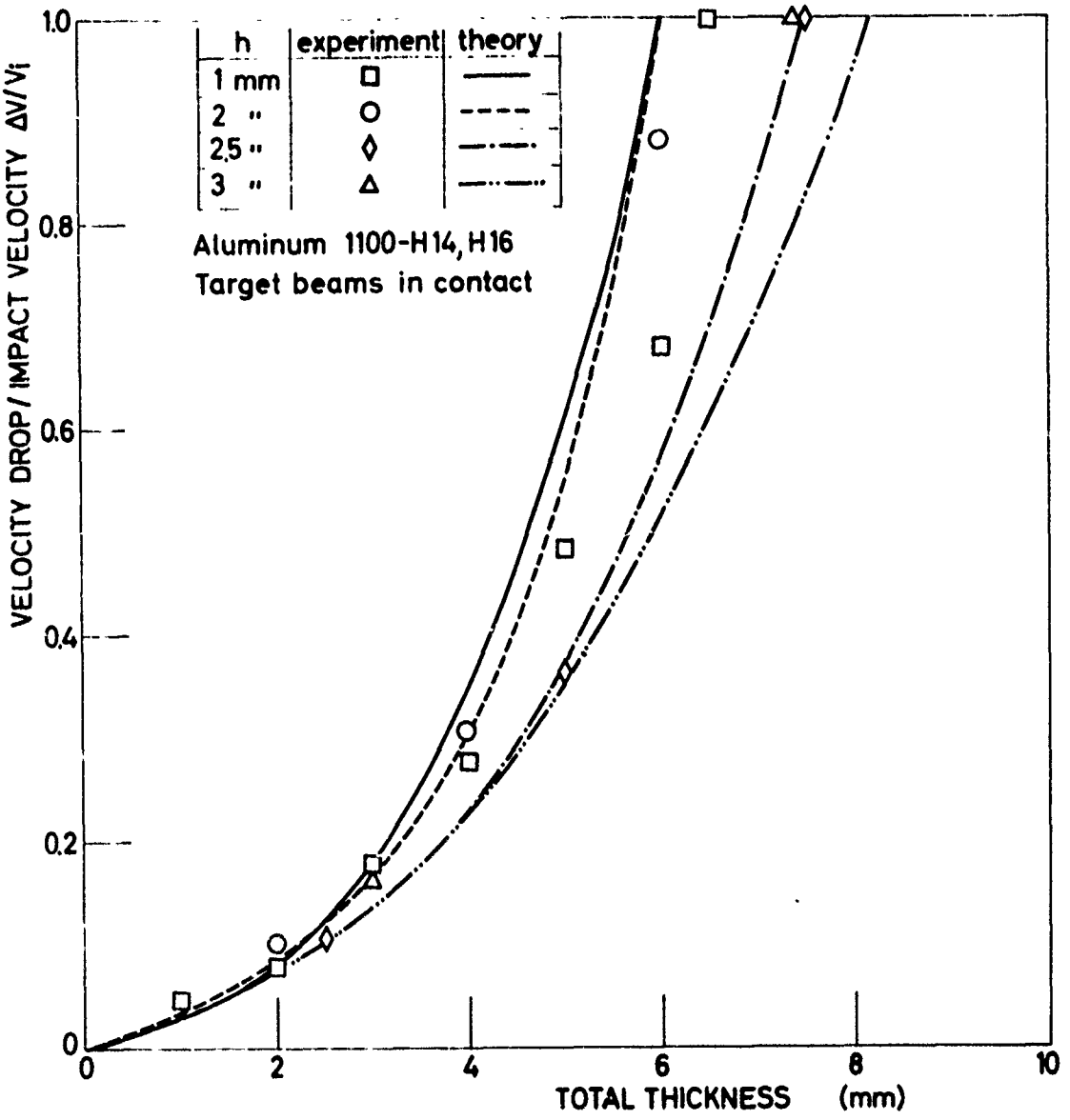
h
experiment
theory
1 mm
2 "
2.5 "
3 "
Aluminum 1100-H14, H16
Target beams in contact
VELOCITY DROP / IMPACT VELOCITY ΔV/Vi
1.0
0.8
0.6
0.4
0.2
0
0
2
4
6
8
10
TOTAL THICKNESS (mm)

FIG. 8

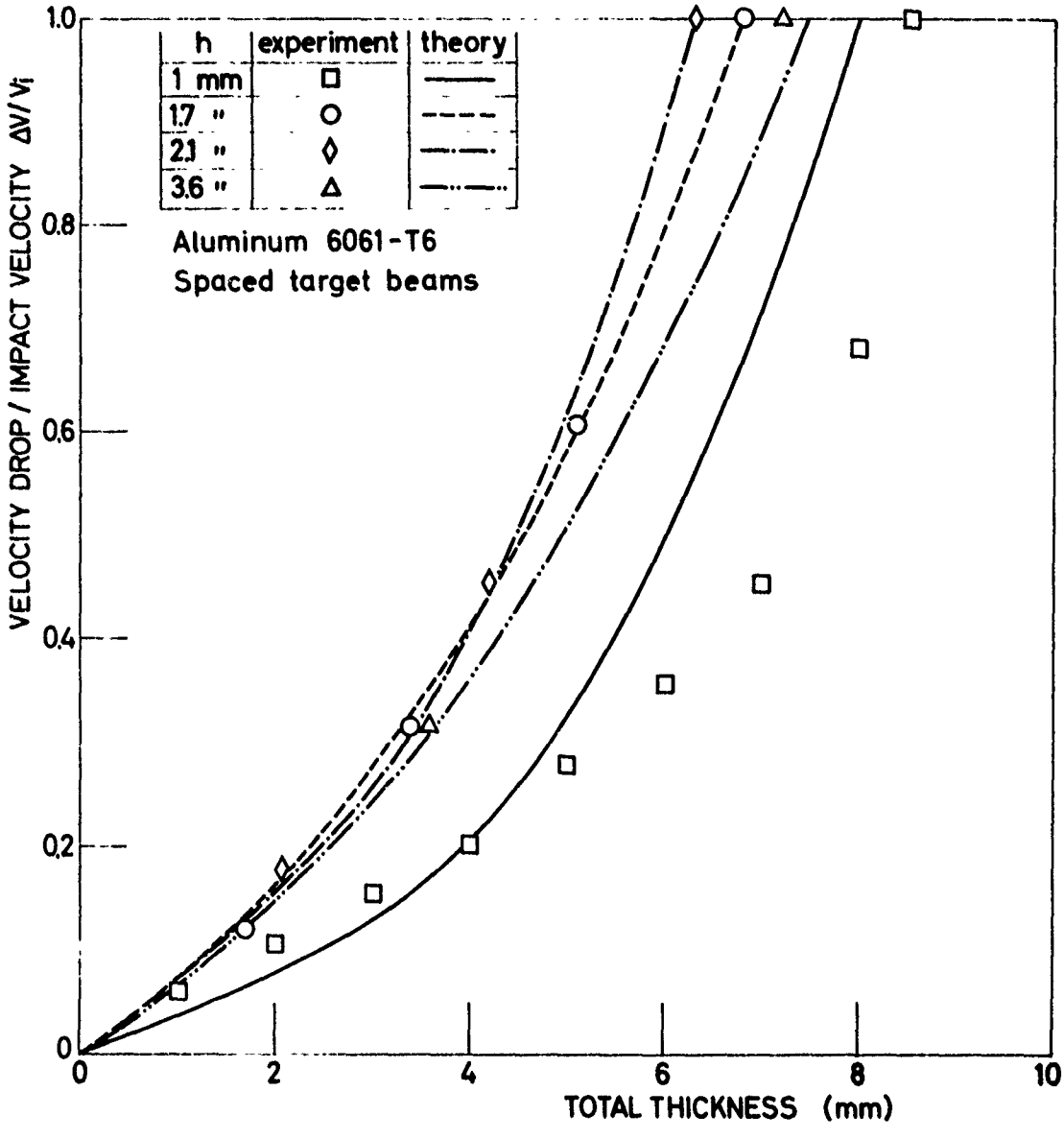
h
experiment
theory
1 mm
1.7 "
2.1 "
3.6 "
Aluminum 6061-T6
Spaced target beams
VELOCITY DROP / IMPACT VELOCITY ΔV/Vi
TOTAL THICKNESS (mm)
0
0.2
0.4
0.6
0.8
1.0
0
2
4
6
8
10

FIG. 9

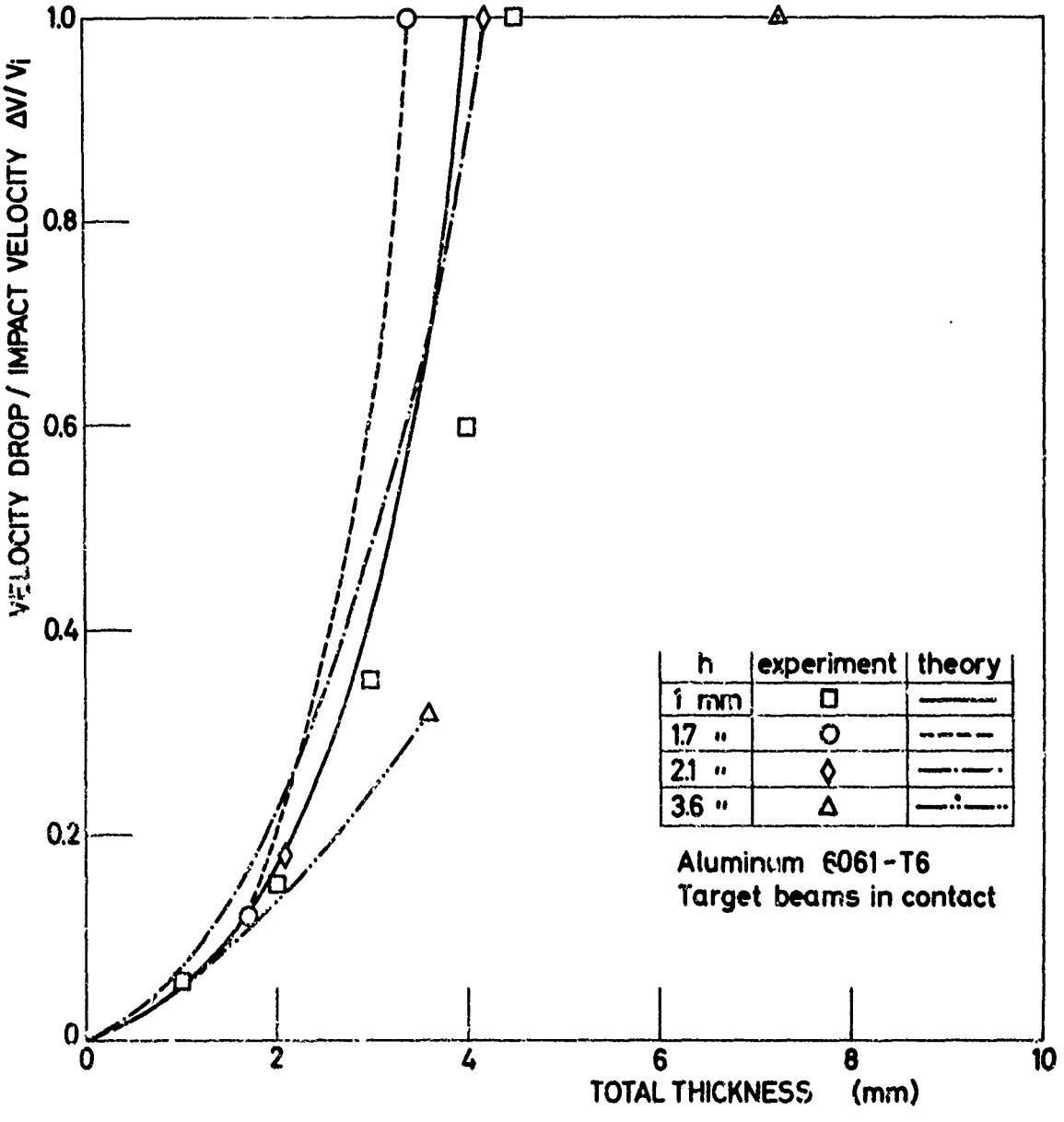
1.0
0.8
0.6
0.4
0.2
0
VELOCITY DROP / IMPACT VELOCITY ΔV/Vi
0
2
4
6
8
10
TOTAL THICKNESS (mm)
h | experiment | theory
1 mm
1.7 "
2.1 "
3.6 "
Aluminum 6061-T6
Target beams in contact

FIG. 10